

John Kong* and Kevin Young

Ultra-smooth finishing of aspheric surfaces using CAST technology

Abstract: Growing applications for astronomical ground-based adaptive systems and air-borne telescope systems demand complex optical surface designs combined with ultra-smooth finishing. The use of more sophisticated and accurate optics, especially aspheric ones, allows for shorter optical trains with smaller sizes and a reduced number of components. This in turn reduces fabrication and alignment time and costs. These aspheric components include the following: steep surfaces with large aspheric departures; more complex surface feature designs like stand-alone off-axis-parabola (OAP) and free form optics that combine surface complexity with a requirement for ultra-high smoothness, as well as special optic materials such as lightweight silicon carbide (SiC) for air-borne systems. Various fabrication technologies for finishing ultra-smooth aspheric surfaces are progressing to meet these growing and demanding challenges, especially Magnetorheological Finishing (MRF) and ion-milling. These methods have demonstrated some good success as well as a certain level of limitations. Amongst them, computer-controlled asphere surface-finishing technology (CAST), developed by Precision Asphere Inc. (PAI), plays an important role in a cost effective manufacturing environment and has successfully delivered numerous products for the applications mentioned above. One of the most recent successes is the Gemini Planet Imager (GPI), the world's most powerful planet-hunting instrument, with critical aspheric components (seven OAPs and free form optics) made using CAST technology. GPI showed off its first images in a press release on January 7, 2014. This paper reviews features of today's technologies in handling the ultra-smooth aspheric optics, especially the capabilities of CAST on these challenging products. As examples,

three groups of aspheres deployed in astronomical optics systems, both polished and finished using CAST, will be discussed in detail.

Keywords: free form optics; light weight SiC aspheres; optics for adaptive optics; precision asphere; ultra-smooth aspheres fabrication.

DOI 10.1515/aot-2014-0015

Received February 27, 2014; accepted May 6, 2014

1 Introduction

The new generation of astronomy telescopes, spectrographs and planet finder coronagraphs are designed with adaptive optics methods. Besides the active optics itself, aspheric optics and/or non-axisymmetric optics require complex surface designs or ultra-smoothness and finishing accuracy, most times the combinations of the both. Conventional optics fabrication is limited by surface form complexity and/or accuracy. The state-of-the-art technologies allow for obtaining highly accurate aspheric shapes, but require pre-polishing processes to overcome the high and mid-spatial frequency errors (MSFR) introduced by the sub-aperture tool marks of grinding.

Scattering from optical fabrication errors frequently dominates both diffraction effects and residual design limitations in their effect upon image quality. In particular, scattering from mid-spatial frequency optical fabrication errors severely degrades system resolution, especially at the very short X-ray/EUV wavelengths.

Solar studies or air-borne optics systems used in satellite tracking applications employ lightweight SiC materials [1]. With the hardness of SiC being similar to diamond, conventional polishing methods suffer from slow material removal rates, difficulty in achieving the desired figure and inherent risk of causing catastrophic damage to the lightweight structure [2].

Various fabrication techniques for finishing ultra-accuracy and ultra-smooth aspheric surfaces have been

*Corresponding author: John Kong, Precision Asphere, Inc., 48860 Milmont Drive, Unit 105-C, Fremont, CA 94538, USA, Tel.: +510-668-1508, Fax: +510-668-1595, e-mail: jkong@precisionasphere.com

Kevin Young: Precision Asphere, Inc., 48860 Milmont Drive, Fremont, CA 94538, USA

proposed and discussed elsewhere [3–10]. This paper reviews the manufacturing capabilities of various technologies, among them, computer-controlled asphere surface-finishing technology (CAST), developed by PAI, a computer numeric control (CNC)-Pitch sub-aperture surface finishing technology, on these challenging products.

2 Ultra-smooth asphere manufacturing technologies

2.1 Mid-spatial frequency error and surface microroughness

In an adaptive optics system, the deployment of an active mirror compensates for the imaging error caused by the air turbulence. The ever-increased number of channels of the active mirror can also be used to correct, to a certain level, the imaging errors caused by imperfection of other optics in the system. This correction, however, is limited to the relatively low spatial frequency surface irregularities, traditionally referred to as ‘figure’, of the optics surface. Active optics cannot correct or compensate for high and MSFR in the optics train.

While high spatial frequency finish errors scatter energy out of the image core into a broad scattering halo, again without significantly broadening the image core, the mid-spatial frequency surface irregularities produce small-angle scatter which has the effect of smearing out the image core, thus reducing the resolution drastically [11].

MSFRs are either caused by the geometry of the grinding or polishing tools, or caused by parameters including the geometry of the motion path of the tool, overlap in the programmed path, motion control instability, motion control overshoot (accelerations and decelerations), vibration in the finishing machine, tool chatter, tool wear instability, polishing tool deformation, cyclical tool wear, and work piece deformation such as can be observed as face-sheet print-through from rib structures in lightweight optics. When finishing hard materials like air-born optics made of SiC, causes of mid-spatial errors relating to tool wear, tool deformation, and tool chatter/vibration can be more pronounced due to the increased hardness of the material. Therefore, obtaining a low MSFR means a systematic or artistic-like control and balance of all the optics producing processes and tools.

High spatial frequency error, usually referred to as surface micro-roughness (SR), is mostly influenced by the

surface contact matching of polishing pad and optics substrate, and their interaction with polishing compound.

The surface characteristics of optics are evaluated by the following parameters: surface figure [peak to valley (PV) and/or RMS]), mid-spatial frequency surface irregularity, slope errors, and SR. It is important to meet all parameters during the product manufacturing; amongst them the mid-spatial frequency error (MSFR) and SR are crucial to the performance of the optics systems, especially for adaptive optical systems, where low spatial frequency error can be mostly, if not all, compensated by the active mirror.

Aspheres in applications such as exoplanet imaging or adaptive optics systems, as well as solar studies and airborne optics systems, require sub-nanometer mid-spatial frequency surface irregularity MSFR ($<10 \text{ \AA}$ RMS) and an SR of better than $<5 \text{ \AA}$. This means that the surface must have atomic level accuracy and smoothness.

2.2 MRF and ion-milling aspheric surface finishing

MRF [12] and ion-milling [13] provide successful state-of-the-art asphere surface finishing technologies. The MRF process routinely polishes surfaces to so-called ‘super polish’ leaving microroughness of the surface (parameter R_a) well below 1 nm [10]. The Ion-Milling method has demonstrated the capability to finish an aspheric surface with figure accuracy as low as 180 pm RMS [3].

It is also important to note that both technologies have low material removal efficiency. Ideally, most of the material should be removed with an asphere generator. The final polishing run is where MRF and ion-milling are best used. However, the process of the asphere generator is one of the major origins of mid-spatial and high-spatial frequency errors, not the least of which are created by the use of small area tools traversing over defined paths to generate an aspheric form. These tool-induced errors can be difficult or impossible to remove (especially by MRF and ion-milling methods), as they often persist deep into the surface and subsurface, especially on hard ceramic materials such as SiC [14].

2.3 CAST technology: ultra-smooth aspheric surface finishing

CAST incorporates conventional pitch polishing processes into a modern CNC platform to achieve a deterministic surface figuring while yielding near super-polished

surface smoothness. The innovative way of applying polishing pressure and controlling tool path enables the suppression and elimination of mid-spatial frequency surface irregularity. It offers a combination of the following features into one machine.

2.3.1 Deterministic process resulting in fast convergence of surface figure

PAI's CAST technology consists of a CNC platform, house-specific software, and associated processes. The CNC platform has been constructed using a precision positioning system with commercially available, customizable mechanical components. The polishing head is attached to a pressure-sensitive arm that is mounted on gantry stages. A sub-aperture tool is moved across the optical surface radially (3-axis mode), while the part to be polished is mounted on a variable speed spindle for circularly symmetric optic. The system also operates in 5-axis mode, where raster motion of the polishing head over optical surface allows for generating, polishing and figuring of rotationally asymmetric features.

The relative dwell time of the tool over a given position is calculated using a mathematical algorithm based on its deviation from nominal figure, the pressure of tool applied on the part, and other machine operating parameters that are also controlled. By varying the amount of time the machine works on any region, a controlled amount of material will be removed. The best tool configuration for any polishing/figuring operation is determined by use of computer modeling, while the proper operation parameters are obtained from experimentation.

After testing of various polishing pressures and measuring resulted material removal rates and SR, the material removal rate data will be incorporated into a deterministic motion control calculation. Using suitable polisher composition materials, customized design of polishing pad, and careful selection of polishing agents, CAST process is optimized for targeted surface polishing and figuring of a particular optics configuration. This technology has proven successful in meeting or exceeding surface figure and finishing specifications, while delivering on targets of cost and schedule.

2.3.2 Fast material removal rate

The polishing tool provides a key element for fabricating aspheric surfaces [15]. CAST uses different materials (natural and man-made), or a combination of several types

of materials, to form the polishing tool pads. Their sizes can range from 1 mm to 100 mm. Many factors, including size of the optic, aspheric surface shape, its maximal departure from best-fit-sphere, substrate material's hardness, volume of material to be removed, and surface finish requirement, will influence the selection of polishing pad geometry and material composition. The goal is to achieve the best material removal rate and polishing stabilities suitable for the particular stage of the processes.

We have achieved fast material removal rates that allow us to economically aspherize glass substrates with over 100 microns of aspheric departure without roughening up the surface. For example, at 1 mm³/min removal rate, we aspherized a 100 mm diameter fused silica part with 100 microns aspheric departure, resulting a 0.3 microns PV smooth surface. It also had shown effectiveness at removing surface pits and scratches. In addition, CAST technology's material removal rate on SiC has reached a level where it is comparable to that of fused silica.

2.3.3 Ultra-smooth finish

CAST was designed to accommodate polishing pads of various shapes, sizes, and material. This ability to have a large selection of polishing tools coupled with a polisher spindle design for easy interchangeability, allows us to quickly switch back and forth between figuring and finishing pads. For example, pad size needs to be big enough for, but not necessarily bigger than, the lower end spatial wavelength of MSFR region specified for the application. The pitch pad, incorporated with a predication algorithm, is especially useful in enabling us to yield ultra-smooth surfaces without significant degradation of surface figure at the finishing process stage.

CAST's surface finishing process can yield a figured surface as smooth as 'within a few times the size of an atom' (http://www.upi.com/Science_News/2014/01/07/Planet-hunting-telescope-camera-returns-first-images-of-exoplanets/UPI-67751389129075/), with mid-spatial frequency surface irregularity <5 Å RMS and SR <2 Å RMS.

2.3.4 No introduction of proprietary polishing agent

CAST technology uses conventional polishing agents and achieves excellent results by tightly controlling their physical and chemical properties. However, this is done without introducing any non-conventional substances or chemicals, which might not be compatible with certain

application environments. For example, we can incorporate well-developed polishing agents and processes used on flat and spherical optics for super-high power laser optics into our aspheric surface finishing process, avoiding proprietary compounds containing ferric particles which lower the damage threshold of laser optics.

2.3.5 Capability to polish a broad range of substrate materials

It has been proven that CAST technology can be applied to many types of (reflective and diffractive) substrate materials. This capability will be demonstrated in this paper through Zerodur® and SiC substrates. Many other examples, including other glass substrates, aluminum, single crystal silicon, calcium fluoride, etc. will be discussed in separate papers. As a matter of fact, due to its ability to incorporate conventional types of polishing pad materials and agents, CAST technology should be effective in polishing aspheric surfaces on any type of material to a similar level of finish which conventional non-CNC polishing achieves on flat and spherical optics.

2.3.6 Maximum flexibility and manufacturing efficiencies

PAI's in-house developed polishing system with innovative technologies, allows for easy duplication of similar systems with high economic efficiency and maximum flexibility. This is essential for optics made of hard materials like SiC and Sapphire, where the polishing of one optic involves the usage of several agents containing diamond of various sizes. Dedicated machines for a small range of diamond sizes is critical to avoid cross contamination of particles into subsequent process steps. This contamination would cause catastrophic scratch damage on the optic surfaces. At the same time, having multiple machines working together will save processing time, speed up the delivery, and reduce cost of frequent thorough machine cleaning when switching polishing agents in a volume production environment.

2.4 Metrology

Surface metrology data is obtained first by a contact profilometer, Form Talysurf (Taylor-Hobson, UK), which guides the computer controlled polisher to bring the surface shape to within the reach of phase-shifting interferometry. In conjunction with proper null optics [2, 16], full-aperture interferometry is used for final figure and

mid-spatial frequency irregularity correction. Double optical path testing setups enable the test of surface irregularity down to single digits in nm RMS without putting extreme requirements on the null optics and interferometer.

For the final testing results, multiple instruments have to be used to cover different spatial frequency ranges. For optics used in visible and near IR applications, a full-aperture interferometer is used for measuring surface figure and mid-spatial frequency irregularity, a micro-phase-measuring interferometer is used for measuring micro-roughness. For EUV optics, mid-spatial frequency surface irregularity is measured using a micro-phase-measuring interferometer, while a third instrument, atomic force microscopy is used for microroughness measurements.

3 Examples of ultra-smooth aspheric surfaces using CAST

3.1 Aspheres for exoplanet imaging

3.1.1 The GPI's first images of exoplanets

A new instrument, attached to one of the most powerful telescopes in the world, has opened its infrared eye for the first time, taking snapshots of a nearby planet orbiting another star and a ring of proto-planetary stellar dust [17]. The sophisticated car-sized instrument, the GPI is attached to the 8-meter Gemini South telescope in Chile and represents a new era in exoplanetary discovery. See Figure 1 for more details. The GPI, which has been in development since 2003, is capable of not only resolving

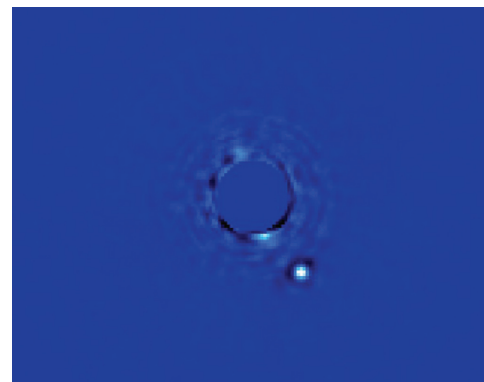


Figure 1 Gemini Planet Imager's first light image of Beta Pictoris b, a planet orbiting the star Beta Pictoris. The star, Beta Pictoris, is blocked in this image by a mask so that its light does not interfere with the light of the planet. (Photo Courtesy Gemini Observatory.)

Table 1 Dimensions and specifications of PAI manufactured glass off-axis aspheres using CAST technology for GPI, resulting in ultra-low mid-spatial frequency surface irregularities.

	GPI-1 (OAP1)	GPI-2 (OAP2)	GPI-3 (OAE1)
Diameter (mm)	50	50	28
Type	Off-axis-parabola	Stand-alone OAP (free-form)	Off-axis-ellipsoid
Aspheric departure (μm)	3	12	5
Surface figure PV (nm)	19 ($\lambda/33$)	19.6 ($\lambda/32$)	16.4 ($\lambda/39$)
Surface figure RMS (nm)	1.87	0.92	1.49
Mid-spatial frequency error (nm)	0.47	0.51	0.28
Micro-Microroughness Ra (\AA)	3	3	3

the dim light from an exoplanet orbiting close to its parent star; it can also analyze the planet's atmospheric composition and temperature. The majority of ground-based exoplanet surveys watch for stars' 'wobbles' to betray the gravitational presence of massive exoplanets in orbit known as the 'radial velocity technique' [18].

3.1.2 Off-axis-parabola (OAP), freeform (stand-alone OAP), and off-axis-ellipsoid (OAE) inside GPI

In this paper, we present three types of ultra-smooth aspheres, selected from among the seven different types in which many copies of each were fabricated by PAI for GPI: an OAP separated from parent mirrors (OAP1), a standalone OAP (OAP2) (a free-form optics), and an OAE (OAE1). Table 1 summarizes one typical example mirror from each type with information of sizes and finished surface parameters.

All optics for the GPI applications used ZERODUR® as mirror substrates. PAI's CAST manufacturing processes

started with the polished best-fit-spheres for all mirrors. Aspherizing, figuring, and final finishing were the three distinguishing processes steps, where different sizes and types of tool pads were used to achieve the best results.

For OAP1 and OAP2, though the polishing machine operation modes were different (radial motion vs. raster motion), we were able to achieve a similar result on surface figure peak-to-valley of around 19 nm ($\lambda/33@633$ nm) and microroughness to about 3 \AA RMS.

Figures 2 and 3 are interferograms of OAP1 and OAP2, showing the most critical specifications of surface figure RMS and mid-spatial-frequency errors. In each figure, the interferogram on the left demonstrates the OAP's surface figure RMS accuracy (as low as 1.87 nm for the OAP1 and 0.92 nm for OAP2); and the diagram on the right shows the mid-spatial-frequency surface irregularities that have been reached (0.47 nm for the parent-separated OAP1 and 0.51 nm for the stand-alone OAP2).

The 28 mm off-axis-OAE elliptical mirror (OAE1) has been finished with a similar surface microroughness and

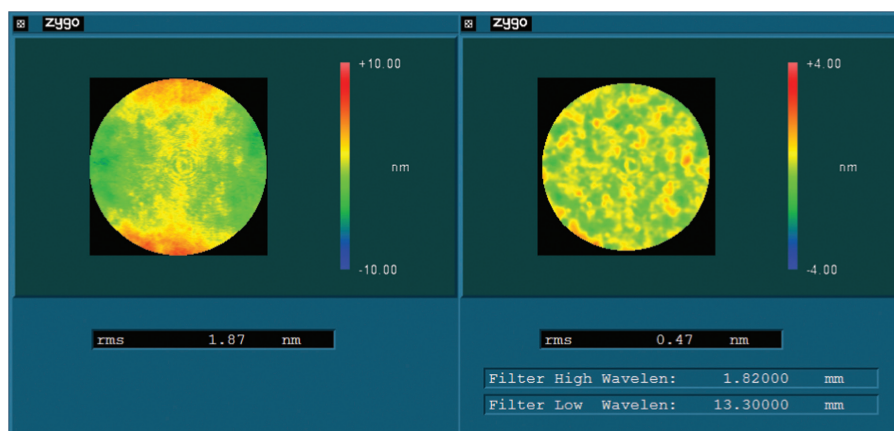


Figure 2 Interferograms of a 50 mm diameter off-axis-parabolic mirror surface (OAP1 from Table 1). The interferogram on the left shows the overall surface figure accuracy RMS=1.87 nm within the clear aperture of 46 mm diameter. The interferogram on the right demonstrates that ultra-low mid-spatial-frequency error has been achieved for this OAP mirror surface (RMS=0.47 nm for the spatial wavelength from 1.82 mm to 13.3 mm, equivalent to spatial frequency range from 0.075/mm to 0.549/mm).

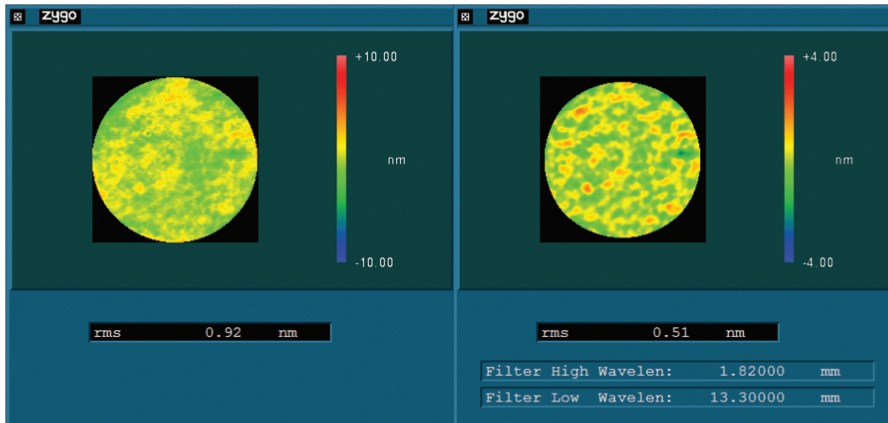


Figure 3 Interferograms of a 50 mm diameter OAP surface (OAP2 from Table 1). This OAP was designed and fabricated as a stand-alone (free-form), not separated from a parent mirror. The interferogram on the left shows the overall surface figure accuracy $\text{RMS}=0.92$ nm within the clear aperture of 45 mm diameter. The interferogram on the right demonstrates that ultra-low mid-spatial frequency error been achieved for this OAP mirror surface ($\text{RMS}=0.51$ nm for the spatial wavelength from 1.82 mm to 13.3 mm, equivalent to spatial frequency range from 0.075/mm to 0.549/mm).

a much lower mid-spatial-frequency error. It has a surface figure peak-to-valley value about 16.4 nm ($\lambda/40$ @ 633 nm) and its mid-spatial-frequency surface irregularity (MSFR) is as low as 0.28 nm. Figure 4 displays the interferograms of the testing results on this OAE. Note again, the interferogram on the left is a result of its surface figure accuracy in RMS and the interferogram on the right demonstrates the quality of mid-spatial-frequency surface irregularity.

Figure 5 is a typical surface microroughness result, representing all seven off-axis-aspheic mirrors fabricated for GPI, taken with a Zygo NewView interferometer (Zygo Corp., USA).

3.2 Aspheres for air-born optics systems and solar studies – SiC substrates

3.2.1 SiC optics

In recent years, SiC has shown to be a material with great promise for general use in optical systems. It has been demonstrated that lightweight SiC mirror substrates can be polished to aspheric shapes and can provide excellent images [4, 19]. The LORRI instrument on New Horizons uses an all-SiC, passively athermal 20 cm telescope to produce high-resolution images [20]. The Herschel

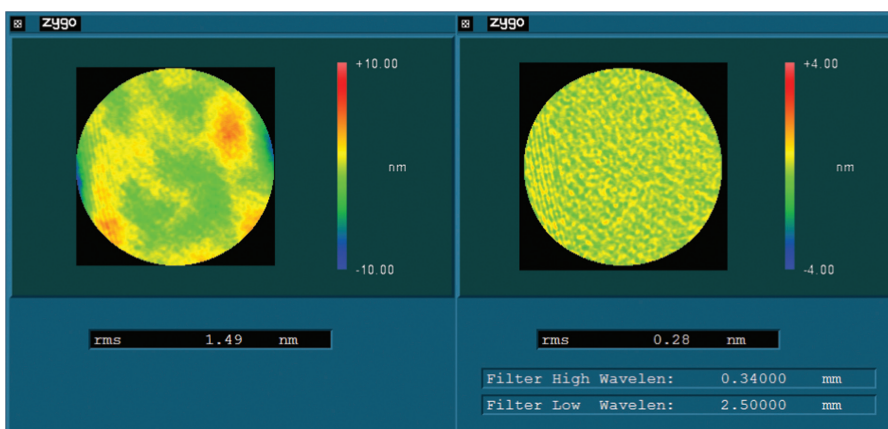


Figure 4 Interferograms of a 28 mm diameter off-axis-ellipsoid surface (OAE1 from Table 1). The interferogram on the left shows the overall surface figure accuracy $\text{RMS}=1.49$ nm within the clear aperture of 26 mm diameter. The interferogram on the right demonstrates that ultra-low mid-spatial frequency error has been achieved for this OAE mirror surface ($\text{RMS}=0.28$ nm for the spatial wavelength from 0.34 mm to 2.5 mm, equivalent to spatial frequency range from 0.40/mm to 2.94/mm).

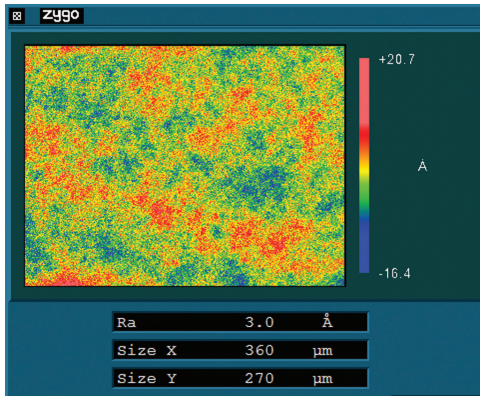


Figure 5 Surface Microroughness of OAE1 measured over 0.36 mm×0.27 mm area using Zygo NewView Interferometer.

Telescope employs a 3.5 m diameter mirror that is composed of 12 SiC petals, brazed together and coated with a thin aluminum reflective coating [21]. To obtain higher imaging and thermal-resolution EUV spectroheliograms, at higher cadence, beyond current capabilities, – it is required to build larger aperture ($D > 30$ cm) multilayer coated optical systems. The advantageous material properties of SiC offer a myriad of opportunities in designing such a telescope.

The primary requirement for obtaining high-resolution EUV images involves the minimization of the surface errors, and surface microroughness.

3.2.2 Results of SiC Aspheres

Three lightweight SiC asphere products delivered to customers are summarized in Table 2. They are all SiC substrates cladded with Chemical Vapor Deposition (CVD-SiC) overcoat layers. Some of them have been employed into air-born optics systems. From the three, two are on-axis convex hyperbolic aspheric mirrors with diameters of 104 mm and 324 mm. The third is an off-axis-parabola SiC

Table 2 Dimensions and specifications of PAI manufactured Silicon Carbide aspheric mirrors using CAST technology, yielding low SR and surface figure parameters to the specifications.

	SiC-1	SiC-2	SiC-3
Diameter (mm)	104	324	159
Type	Convex Hyperbolic	Convex Hyperbolic	Stand-Alone OAP
Aspheric Departure (μm)	20	88	452
F/#	1.35	2.5	1.6
Surface Figure RMS (nm)	12.8	12.3	17.9
Micro-Microroughness Ra (Å)	1.4	3.6	3.4

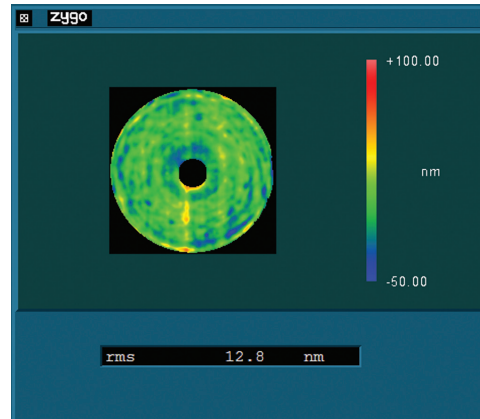


Figure 6 Interferogram of a 104 mm diameter lightweight SiC convex hyperbolic mirror surface (SiC-1 on Table 2). The face sheet thickness is <2 mm and the asphere departure is 20 microns. Finishing specification calls for 1/40 waves RMS@633 nm over the clear aperture of 91 mm, 1/50 waves RMS was actually achieved.

mirror with a diameter of 159 mm, designed and polished as a stand-alone OAP.

Figure 6 show the result of SiC-1, a 104 mm diameter convex hyperbolic mirror with 20 microns aspheric departure from the best-fit-sphere. This mirror is lightweight, constructed with open and ribs supported back. It has a face sheet thickness of <2 mm, which makes it extremely fragile. Therefore, it requires much more sensitive polishing and finishing touches, while maintaining the efficient material removal. The realized thin-face-sheet SiC asphere has a fast ($F/\# = 1.35$) aspheric surface figure and the surface microroughness achieved was <2 Å (microroughness $R_a = 1.4$ Å), as shown in Figure 7. A photograph of this mirror is shown in Figure 8.

The second SiC mirror SiC-2 is a relatively large one, with a 324 mm diameter. The front surface shape is

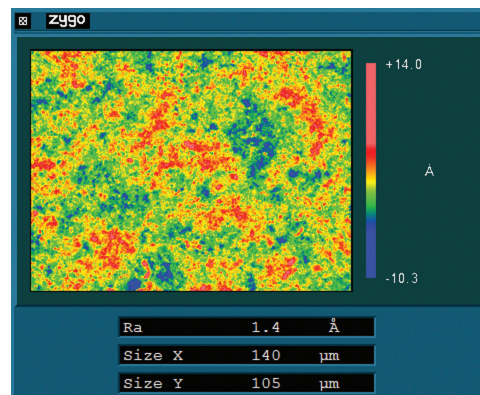


Figure 7 Surface Microroughness of polished SiC-1 surface measured over 0.140 mm×0.105 mm area using Zygo NewView Interferometer.

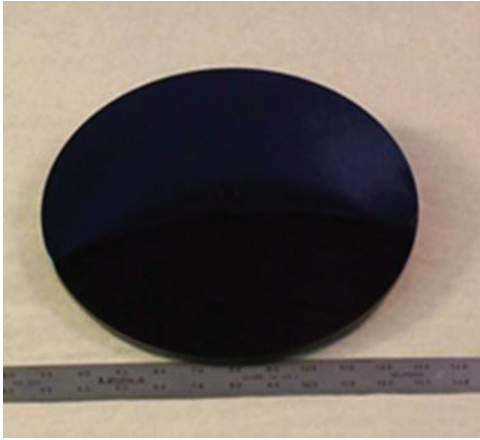


Figure 8 A convex hyperbolic SiC lightweight optic, SiC-1. Diameter: 104 mm; finished figure: $\lambda/50$ waves RMS; microroughness: $<2 \text{ \AA}$ RMS [16].

convex hyperbolic and back surface is lightweight, constructed with open and ribs structure. Face sheet thickness is $<4 \text{ mm}$, with an aspect ratio of 15:1 at the largest crossing area. It has an 88 microns aspheric departure. CAST manufacturing processes finished it with an even lower face figure RMS value (12 nm, as shown in Figure 9). Although it is large in size, the microroughness of this mirror was finished to $Ra=3.6 \text{ \AA}$ RMS.

The third piece is a 159 mm diameter freeform or stand-alone OAP, SiC-3. It has a large asphere departure of 452 μm , and a faster asphere parameter $F/\# = 1.6$. CAST manufacturing process finished the SiC asphere meeting all the specifications required; see Figure 10 for the full

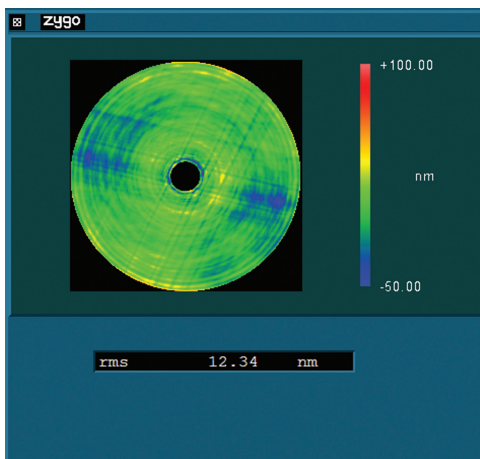


Figure 9 Interferogram of 324 mm diameter lightweight SiC on-axis convex hyperbolic aspheric optics (SiC-2 on Table 2). The face sheet thickness is 4 mm and the asphere departure is 88 m. $F/\# = 1.35$, finished surface accuracy RMS=12.34 nm and microroughness $Ra=3.6 \text{ \AA}$ RMS) over the clear aperture of 308 mm.

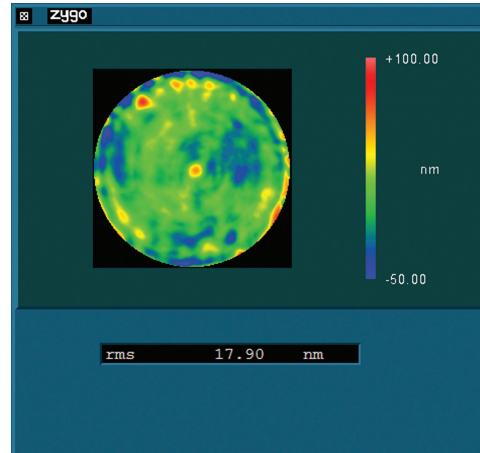


Figure 10 Interferogram of a 159 mm diameter lightweight SiC, which is fabricated as a stand-alone off-axis-parabola (freeform) (SiC-2 on Table 3). It is a rather fast with $F/\# = 1.6$ and large aspheric departure (452 m) from best-fit-sphere. Although the material removal on this hard SiC substrate is large, CAST was able to achieve good result with surface figure=17.90 nm RMS and microroughness $Ra=3.4 \text{ \AA}$ RMS

aperture interferogram. Similar surface microroughness to the large SiC-2 was achieved, this freeform SiC has an impressive microroughness $Ra=3.4 \text{ \AA}$ RMS. A photograph of SiC-3 mirror is shown in Figure 11.

3.2.3 Discussion of SiC asphere fabrication and measurement

PAI's CAST manufacturing processes used to produce lightweight SiC aspheres has a long development history.

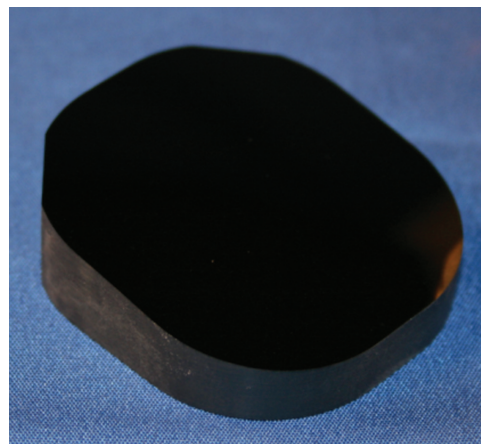


Figure 11 A stand-alone off-axis convex hyperbolic SiC mirror finished to surface figure accuracy of 0.020 waves RMS at 633 nm (SiC-3 on Table 2).

With years of improvement, the processes have become matured and versatile enough for the reliable delivery of industrial mirrors. It offers the following four major advantages:

1. **Fast material removal rate:** By optimizing the pressure applying mechanism and selection of the most suitable polishing pads, CAST technology's material removal rate has reached a level where it is comparable to the material removal rate of glass substrates, such as fused silica.
2. **Minimized 'quilting' effect:** The lightweight mirrors are prone to 'quilting', a type of figure where the cells in the mirror will appear puffed up in the center. The polishing pressure deflects the face sheet at each cell and smoothing the surface. After the tool is lifted, the cells spring up and cause the quilted appearance [22]. Part of the CAST technology used on SiC surface finishing has a special way of applying polishing pressure, such that it will produce lightweight optics with inherently minimal quilting effect in comparison to the mirror's specified figure requirement. This can be seen from the figures shown within this section. The technique works identically well on lightweight glass substrates (this will be demonstrated in a separate paper). In addition, CAST is capable of correcting any residue quilting effect when necessary.
3. **Ultra-smooth surface finish:** A comparison of the surface microroughness of our super-polished SiC substrate to that of a super-polished Zerodur® mirror had been carried out [1, 2]. The result is demonstrated in Figure 12. The Zerodur® mirror is 92 mm in diameter
4. **Best performance-to-cost ratio:** Due to the hardness nature of this material, SiC optics polishing requires various grades of diamond fluids to go through the process steps, from bulk material removal to final microroughness finish. These fluids contain diamonds of different diameters. Cross contamination of the polishing platform poses a major challenge. CAST uses an innovative design to build the polishing platform using easily available customized and off-the-shelf automation components. This cost-effective model allowed us to use multiple platforms, each one dedicated to a range of diamond sizes, to cover the entire process train. The cross contamination risk is then reduced to the lowest achievable, without significantly increasing the cost of capital compared with using otherwise commercially purchased CNC equipment.

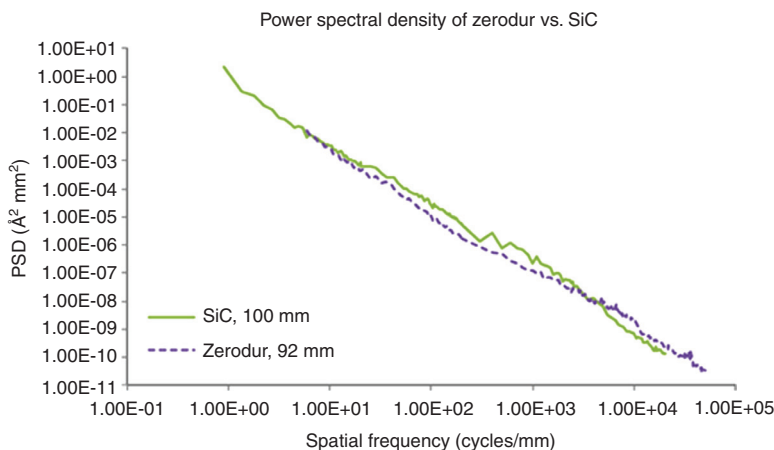


Figure 12 Power density spectrum of a super-polished 100 mm diameter SiC aspheric mirror, in comparison with that of a 92 mm diameter Zerodur® mirror. Over the spatial frequency range from 10 to 104 cycles/mm, the RMS microroughness for each substrate is equal to 3.4 and 2.5 Å, respectively (courtesy of Ref. [2])

3.3 Aspheres for adaptive astronomical telescope systems

3.3.1 Adaptive optics (AO)

AO is a technique that aims at compensating quickly varying optical aberrations to restore the angular resolution limit of an optical system. It uses a combination of wavefront sensors (WFSs), to analyze the light wave aberrations, and phase correctors (e.g., deformable mirrors) to compensate for them [23].

Modern and future astronomical or extremely large telescopes mandate adaptive optical systems. A fast response adaptation of active optics is adaptive optics. Working at fast timescales (0.001 s or less) rapid fluctuations caused by atmospheric turbulence can be compensated real-time [24]. A wavefront sensor measures the distortions that are compensated by a rapidly deformable mirror that counteracts the influence by taking the equivalent shape of the particular distortion. This promising solution of high-order atmospheric turbulence correction is provided by a deformable active mirror in the system. Having one mirror of the telescope train to be adaptive, the whole telescope then becomes an adaptive optical system, offering fast wavefront correction without addition of supplementary optics or mechanics [24].

The adaptive designs open up unexplored possibilities in fundamental astronomical research that allows the design for astronomical telescopes to increase the telescope size and instrumentation complexity with an ever better performance, either for ground-based astronomy or in space. This new generation of giant telescopes and instrumentations needs new developments in terms of technology, performance, and optical surface quality [25]. In the cosmology to exoplanets detection context, the scientific programs push instrument complexity to the edge because the Active Optics methods enable the production

of complex optical surfaces of very high quality. Meanwhile, the next generation of astronomical instrumentation will benefit from the optical quality and adaptive components [26].

As the low-spatial frequency errors are corrected by the active mirror, mid- and high-spatial frequency errors become the dominant specifications for other optics within an adaptive system. GPI mentioned in Section 1 of this paper is an adaptive optics application case on ground-based astronomical instrumentation. PAI's CAST asphere manufacturing ability allows us to provide demanding high precision optics for adaptive astronomical telescope systems. The use of adaptive optics for both the telescope and the instrumentation helped enable CAST processes to further develop and be optimized, by providing the extreme requirements and challenges for delivering higher accuracy aspheres with complex surface designs and super smoothness quality.

3.3.2 Aspheres for astronomy telescope adaptive systems

Table 3 lists three mirror examples used in adaptive optics systems manufactured with PAI's CAST polishing and finishing processes. A 356 mm diameter, stand-alone, large off-axis-hyperbola (ADO-1, stand-alone OAH); a small, stand-alone, 64 mm diameter off-axis-parabola (ADO-2, stand-alone OAP) and a 378 mm diameter large convex, fast ($F/\# = 1.4$) hyperbolic secondary mirror (ADO-3).

While the first two components used Zerodur[®] as substrates the third one is made of Fused Silica. Again, CAST manufacturing performs the aspherization and surface finishing of all the mirrors from their best-fit-spheres. The small 64 mm diameter stand-alone OAP required 1/50 waves@633 nm peak-to-valley surface figure; the other two larger aspheres (OAH and secondary mirror) required a surface with super smoothness and low slope errors.

Table 3 Dimensions and specifications of PAI manufactured low slope error glass aspheres using CAST technology for adaptive optical systems.

	ADO-1	ADO-2	ADO-3
Diameter (mm)	356	64	378
Type	Stand-alone OAH	Stand-alone OAP	Convex hyperbolic
Aspheric departure (μm)	22	19	35
F/#	14.7	3.4	1.4
Surface figure PV (nm)		11.4 ($\sim \lambda/50$)	
Surface figure RMS (nm)	9.4	1.6	5.1
Slope error (μrad)	1.36	1.08	0.57
Micro-microroughness Ra (\AA)	5	5	5

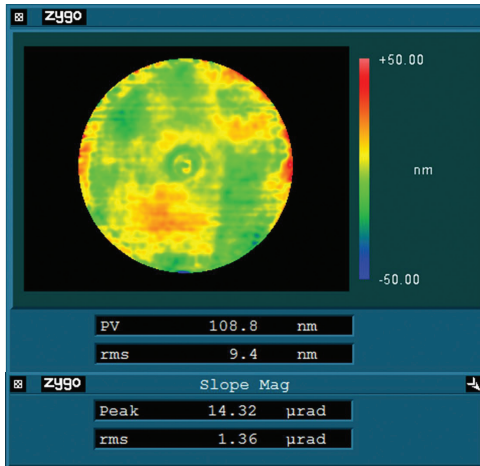


Figure 13 Interferogram of a stand-alone off-axis-hyperbolic mirror (ADO-1 on Table 3, free-form). Mirror size is 356 mm in diameter with clear aperture of 333 mm. The slope error achieved was 1.36 μrad RMS, with surface microroughness of 0.5 nm Ra.

Figure 13 displays the interferogram of ADO-1. This large free form mirror has a low slope error value of 1.4 μRad RMS, meanwhile, the overall microroughness of the surface is as low as half of a nanometer.

Figure 14 shows the small free form mirror (ADO-2). Its finish nevertheless required an ultra-precision peak to valley, with a surface figure RMS of 1.6 nm.

Figure 15 shows the interferogram result of the large convex hyperbolic secondary mirror (ADO-3). The surface design for this large mirror required a larger (30% more

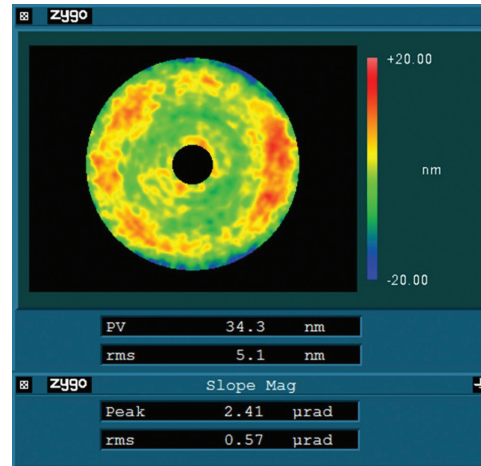


Figure 15 Interferogram of the large secondary mirror (ADO-3 on Table 3). Mirror size is 378 mm in diameter with a clear aperture of 360.2 mm. The slope error achieved was 0.57 μrad RMS, with surface microroughness 0.5 nm Ra.

compared to the 356 mm OAH) asphericity from its best-fit-sphere, and an almost 10 times faster aspheric surface change ($F/\#=1.4$ compared to the other large OAP with $F/\#=14.7$) However, this piece was delivered meeting the specifications with an even more improved slope error (as low as 0.57 μrad RMS), meanwhile, with no compromise to the surface smoothness, a surface microroughness (0.5 nm Ra) has been achieved for this piece.

4 Conclusion

The new generation of astronomical telescopes and instruments of both adaptive ground and air-born systems requires manufacturing support that is equipped with extremely smooth surface finishing capabilities for fabrication of optics components. State-of-the-art technologies that can produce accurate aspheres are often limited either by material removal efficiencies; or by the difficulties of crucial high- and mid-spatial frequency errors due to the conventional sub-aperture aspherization tools

This paper reviewed the capabilities of CAST technology in these challenging application areas. As examples, real deployed optics using CAST have been discussed in detail with both of their polishing and measurement methodologies as well as their results. The products may use materials of almost all types of glasses, glass ceramics (Fused Silica, Zerodur®, ULE, Clear Ceram), single crystal types Si, light weight SiC. Products sizes range from 10 mm to 650 mm in diameter. Optic shapes include

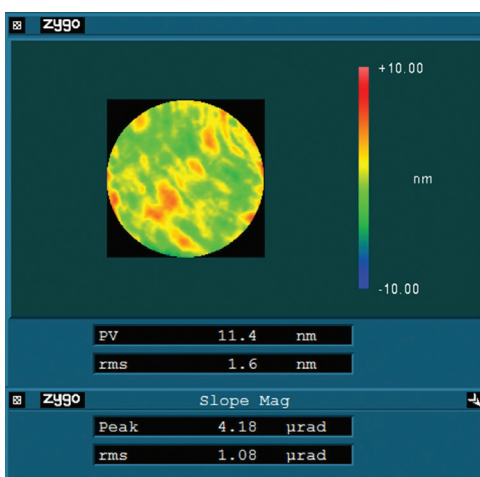


Figure 14 Interferogram of a small stand-alone free-form OAP mirror (ADO-2 on Table 3, free-form). Mirror size is 64 mm in diameter with a clear aperture of 55.8 mm. The surface figure PV value reached 1/50 wave@633 nm, with surface figure RMS of 1.6 nm and slope error of 1.08 μrad RMS. SR was 0.5 nm Ra.

on- and off-axis aspheres, free-form aspheres, achieving surface figure peak-to-valley of 1/50 waves @633 nm, slope error <1 μ rad, and microroughness <2 \AA .

Future astronomy based optical designs will involve the implementation of active and adaptive optics from x-ray to the infrared [27], also the next generation ground and space-based EUV imager has a continuing need to improve observational capabilities at EUV wavelengths in order to obtain higher thermal, spatial and temporal resolution of the solar atmosphere [2]. To better serve both astronomy x-ray and EUV application areas, asphere manufactures need further optimization of the polishing capabilities for both the figure accuracy and surface smoothness. Although CAST demonstrated impressive manufacturing capabilities on surface finishes as smooth as <2–3 \AA for a wide range of extremely high quality aspheres of all materials, we are working on further technology improvement to reach the goal of 1 \AA surface microroughness. In addition, we believe that there is a big potential to combine ion-milling figuring process with CAST, to improve the figure accuracy of larger optics to a higher level in order to deliver significantly improved astronomy X-ray and EUV optics.

Acknowledgments: The authors wish to thank the GPI team (Lawrence Livermore National Lab, Hertzberg Institute of Astronomy, and other institutions), Boeing LTS, Space and Airborne Systems of Raytheon Company, Lockheed Martin Advanced Technology Center, and Trex Enterprises Corporation, for their support in various projects of which those results were presented in this paper.

References

- [1] D. Martínez-Galarce, P. Boerner, R. Soufli, J. Harvey, M. Bruner, et al., “Recent Advances in EUV Optics for use in Solar Physics,” 2nd International Conference on Space Technology (ICST), Sept. 15–17, 2011.
- [2] J. Kong and K. Young, “Optical Finishing of Lightweight Silicon Carbide Asphere Using Sub-Aperture Polishing Technology style,” The 5th SPIE International Symposium on Advanced Optical Manufacturing and Testing Technologies (AOMATT), April 26–29, 2010.
- [3] H. Takino, M. Kanaoka and K. Nomura, “Ultraprecision Machining of Optical Surfaces”, <https://www.jspe.or.jp/english/sympo/2011s/2011s-1-2>.
- [4] M. Fruit, P. Antoine, J. -L. Varin, H. Bittner, M. Erdmann, in ‘Airborne Telescope Systems II’, Ed. By R. K. Melugin, H-P Roeser, Proc. of SPIE, 4857, 274–285 (2003).
- [5] H. Takino, N. Shibata, H. Itoh, T. Kobayashi, K. Nemoto, et al., Appl. Opt. 45, 23 (2006).
- [6] D. Golini, W. I. Kordonski, P. Dumas and S. Hogan, Proc. SPIE 80, 3782 (1999).
- [7] A. Schindler, T. Haensel, D. Flamm, W. Frank, G. Boehm, et al., Proc. of SPIE, 217, 4440 (2001).
- [8] D. D. Walker, A. T. H. Beaucamp, V. Doubrovski, C. Dunn, R. Evans, et al., Proc. of SPIE 6273, 627309-1 (2006).
- [9] M. Kanaoka, C. Liu, K. Nomura, M. Ando, H. Takino, et al., J. Vac. Sci. Technol. B, 25, 2110 (2007).
- [10] S. Gogler, G. Bieszczad and M. Krupiński, Photon. Lett. Poland 5, 128–130 (2013).
- [11] A. Krywonos, J. E. Harvey and N. Choi, JOSA A 28.6, 1121–1138 (2011).
- [12] Chris Supranowitz, Paul Dumas, Tobias Nitzsche, Jessica DeGroot Nelson, Brandon Light, et al., Proc. of SPIE, 8884, 888411 (2013).
- [13] Podzimek, L. H. Beckmann, J. A. Brok, Proc. of SPIE, 0655 (1986).
- [14] R. W. Bin, G. Saurav, L. Xichun, R. J. Millar, Proc. Insti. Mech. Eng., Part B: J. Eng. Manufact. 227, 338–342 (2013).
- [15] J. H. Burge, B. Anderson, S. Benjamin, M. K. Cho, K. Z. Smith, et al., “Development of optimal grinding and polishing tools for aspheric surfaces,” Proc. SPIE 4451, Optical Manufacturing and Testing IV, 153 (December 27, 2001).
- [16] J. Kong, K. Young, “Super Polishing of SiC Aspheric Optics,” [www.opticsinfobase.org > Conference Papers > OFT > 2012 > OW1D?](http://www.opticsinfobase.org/ConferencePapers/OFT/2012/OW1D?)
- [17] P. Michaud, P. Michaud, J. R. Graham and M. Perrin, “Gemini Observatory Press Release,” <http://www.gemini.edu/node/12113>, For Embargoed Release at 10:30 a.m. EST (5:30 a.m. HST), January 7, 2014.
- [18] S. Parimucha, P. Skoda, “Comparison of selected methods for radial velocity measurements,” Proceedings IAU Symposium, No. 240, 2006.
- [19] H. Kaneda, T. Nakagawa, K. Enya, T. Onaka, “Cryogenic optical testing of SiC mirrors for ASTRO-F and C/SiC composite mirrors for SPICA,” in ‘Proc. of the 5th International Conf. on Space Optics (ICSO 2004)’, Ed. By B. Warmbein, ESA SP-554, 699–706, (2004).
- [20] S. J. Conard, F. Azad, J. D. Boldt, A. Cheng, K. A. Cooper, et al., Proc. SPIE, 5906, 407 (2005).
- [21] Y. Toulemont, T. Passvogel, G. Pillbrat, D. de Chambure, D. Pierot, et al., “The 3,5m All SiC Telescope for Herschel”, Proc. Of the 5th International Conf. on Space Optics (ICSO 2004), Ed. By B. Warmbein, ESASP-554, 341-348, 2004.
- [22] B. K. Smith, J. H. Burge and H. M. Martin, “Fabrication of large secondary mirrors for astronomical telescopes.” Optical Science, Engineering and Instrumentation’97. International Society for Optics and Photonics, 1997.
- [23] F. Rigaut, B. Neichel, M. Boccas, C. d’Orgeville, F. Vidal, et al., Mon. Not. R. Astron. Soc. 000, 1–17 (2013).
- [24] G. Kroes, A. Jaskó, J. H. Pragt, L. Venema, M. De Haan, Proc. of SPIE, Vol. 8450, 845029 (2012).
- [25] E. Hugot, M. Ferrari, A. Riccardi, M. Xompero, G. R. Lemaître, et al., Astronomy and Astrophysics 527, 4 (2011).
- [26] J. -G. Cuby, E. Prieto, M. Ferrari, E. Hugot, J. Bland-Hawthorn, et al., “On the performance of ELT instrumentation,” Proc. SPIE 6269, Ground-based and Airborne Instrumentation for Astronomy, 62691U (June 29, 2006).
- [27] G. R. Lemaître, Opt. Rev. 20, 103–117 (2013).



John Kong is the co-founder of Precision Asphere Inc. in Fremont, California, USA, and has served as President of PAI since May 2002. He received his Doctorate (PhD) in Physics from the Institute of Physics, University of Heidelberg, Germany. Prior to founding PAI, John worked in engineering and management in various industries, such as electronics, telecommunication, and semiconductor equipment. His research interests center on improving the understanding, design, and performance of state-of-the-art industrial asphere fabrication and production technologies and capabilities. He is the co-inventor of CAST aspherization and surface finishing technology and successfully implemented CAST in the last decade at Precision Asphere Inc., in the design and manufacturing of high precision custom aspheres for customers worldwide.



Kevin Young is the co-founder of Precision Asphere Inc. in Fremont, California, USA. He has served as the Vice President of PAI since May 2002. He received his Bachelor of Science in Physics from University of Toronto, Canada. He is the co-inventor of CAST technology. He overlooks the company's operation and has about 20 years of experiences in the custom aspheric optics industry.